Dynamics of a relativistic charged particle in a constant homogeneous magnetic field and a transverse homogeneous rotating electric field

A. Bourdier*
Commissariat à l'Energie Atomique, DPTA, Boîte Postale 12, 91680 Bruyères-le-Châtel, France

M. Valentini and J. Valat
Laboratoire de Physique des Milieux Ionisés, Ecole Polytechnique, Centre National de la Recherche Scientifique, 91128 Palaiseau Cedex, France

(Received 18 September 1995; revised manuscript received 3 July 1996)

The relativistic motion of a charged particle in a homogeneous time-independent magnetic field and a transverse circularly polarized homogeneous electric field is reduced to an integrable form. Using canonical transformations, it is shown that the equations of motion can be derived from a one degree of freedom time-dependent Hamiltonian that has a first integral. The trajectories and the dynamics of the particle are studied. Tractable approximate expressions for the maximum kinetic energy are derived in two situations of experimental interest. [S1063-651X(96)09411-1]

PACS number(s): 41.75.−i

I. INTRODUCTION

The charged particle motion in a constant homogeneous magnetic field and a transverse electric field is studied. This problem has already been explored by other authors [1–3]. Roberts and Buchsbaum [1] investigated the relativistic motion of a charged particle in the field of a homogeneous plane electromagnetic field. For the case when the index of refraction is unity, they considered a charged particle that starts from rest in the field of a circularly polarized plane wave whose frequency is equal to the rest mass cyclotron frequency ($eB_0/_m$). They found a ''synchronous'' solution in which the particle gains energy indefinitely. This solution occurs because the particle gains energy parallel to, as well as perpendicular to, the direction of propagation of the circularly polarized plane wave. The increase in perpendicular energy lowers the cyclotron frequency of the charged particle, while an increase in parallel energy changes the velocity of the particle, which results in a Doppler shift to a lower frequency as ''seen'' by the particle. In this case, the Doppler shift to the lower frequency equals the reduction in the cyclotron frequency and the particle remains synchronously in the cyclotron-resonance condition. Hakkenberg and Weening [2] studied the relativistic equation of motion in a constant homogeneous magnetic field and a homogeneous rotating electric field perpendicular to each other. By using the Lorentz equation in the momentum space they have expressed exactly the time dependence of the energy of a particle in terms of elliptic integrals. The maximum energy reached by the particle is calculated numerically for different situations. So, in these two papers [1,2], the integrability of the system is shown by using Lorentz equation as a force equation. Jory and Trivelpiece [3] have studied rather the effects of the spatial variations of the electromagnetic wave field and the steady magnetic field. These studies were done to determine the maximum energy gain for a charged particle in a section of waveguide or a cavity resonator immersed in a steady magnetic field and an electromagnetic wave as a function of the various parameters.

In this paper, the case of a circularly polarized standing wave is considered in order to investigate effects similar to those that might occur in a cavity resonator in which a low-density ionized gas has been created. One of the aims of this work is to bring some enlightenment to the discussions performed in the previous articles by using the Hamiltonian formalism. Another aim is to derive simple approximate expressions for the maximum energy the particle can reach. This gives the upper limit in frequency of the x rays emitted when an electron immersed in the considered electromagnetic wave hits a high-Z material target.

The energy of the charged particle is supposed to be low enough so that dissipation due to radiation can be neglected. As a consequence, the Hamiltonian formalism can be used.

Two constants of motion are obtained simply by integrating the equations of Hamilton. Another constant of motion is derived using Noether's theorem [4,5]. Canonical transformations permit one to reduce the problem to a time-dependent problem with one degree of freedom [6]. The system is shown to be integrable by two different methods. One of them is peculiar to the Hamiltonian formalism; it can be shown that Liouville's theorem still applies in this case [7–9].

The Hamiltonian formalism gives some insight to the discussion concerning the numerically calculated trajectories corresponding to different situations that are shown. It enables one to obtain for them a simple analytic approximate expression that enables one to predict their aspect. For low initial energies of the particle and low values of the electric field the trajectory spirals outward and inward. When the initial energy is high and the electric field low, the trajectories become close to circles.

An equation governing the energy of the charged particle

*Also at Laboratoire de Physique des Milieux Ionisés, Ecole Polytechnique, Centre National de la Recherche Scientifique, 91128 Palaiseau Cedex, France.

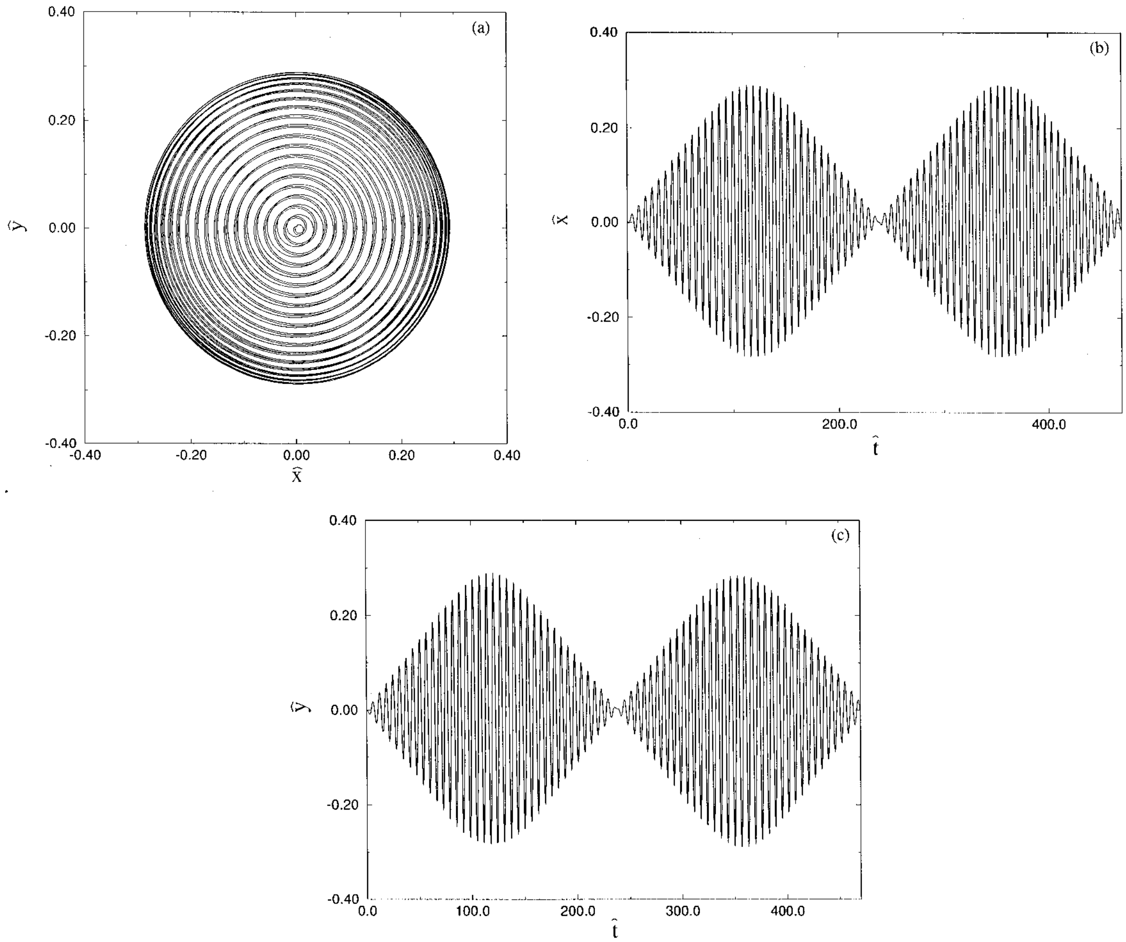

FIG. 1. (a) Trajectory of a charged particle initially resonant and at rest ($\gamma_0=\Omega_0=1$) at $\hat{x}_0=\hat{y}_0=0$ (initial values of $\hat{x}$ and $\hat{y}$) in the $\hat{x}$-$\hat{y}$ plane. $a=3\times10^{-3}$. (b) $\hat{x}$ component of the charged particle in the same conditions as those of (a). (c) $\hat{y}$ component of the charged particle in the same conditions as those of (a).

is derived. It is shown that when the particle is initially at rest, its energy oscillates between two values. Simple approximate expressions for the maximum kinetic energy of the particle are derived when the particle is initially either resonant or ''antiresonant'' (with the magnetic field in the opposite direction). The validity of the expression corresponding to the first situation is discussed by a comparison with the maximum values of the energy obtained by solving numerically the exact energy equation. The importance of taking the magnetic field in the right direction is emphasized. The condition for which a particle initially at rest reaches the maximum possible energy is established.

II. HAMILTONIAN STRUCTURE OF MOTION AND TRAJECTORIES

A. Research of constants of motion: Numerical resolution of Hamilton's equations

The constant magnetic field $\mathbf{B}_0$ is assumed to be along the z axis and the electric field has the components

$$E_x=E_0\cos\omega_0 t,\quad E_y=E_0\sin\omega_0 t,\quad E_z=0, \tag{1}$$

where E_0 and ω_0 are constants. The following gauge is chosen for the electromagnetic field:

$$\mathbf{A}=-\left(\frac{B_0}{2}\,y+\frac{E_0}{\omega_0}\sin\omega_0 t\right)\hat{\mathbf{e}}_x+\left(\frac{B_0}{2}\,x+\frac{E_0}{\omega_0}\cos\omega_0 t\right)\hat{\mathbf{e}}_y. \tag{2}$$

Because of the Maxwell equations, the electric field and the total magnetic field cannot be constant along the z axis. Still, for long wavelengths the additional magnetic field can be neglected in a region where the electric field is maximum; in this domain the given treatment is exact.

The motion of the charged particle is assumed to be in the x-y plane and its relativistic Hamiltonian expressed in mks units is

$$H=\left[\left(P_x-\frac{eE_0}{\omega_0}\sin\omega_0 t-\frac{eB_0}{2}\,y\right)^2c^2+\left(P_y+\frac{eE_0}{\omega_0}\cos\omega_0 t+\frac{eB_0}{2}\,x\right)^2c^2+m^2c^4\right]^{1/2}, \tag{3}$$

where $-e$ and m are the charge and the rest mass of the particle. The very different physical behavior of the nonrelativistic motion is studied in the Appendix. The Hamilton equations allows us to readily find two constants of motion

$$C_1=P_x+\frac{eB_0}{2}\,y,\quad C_2=P_y-\frac{eB_0}{2}\,x. \tag{4}$$

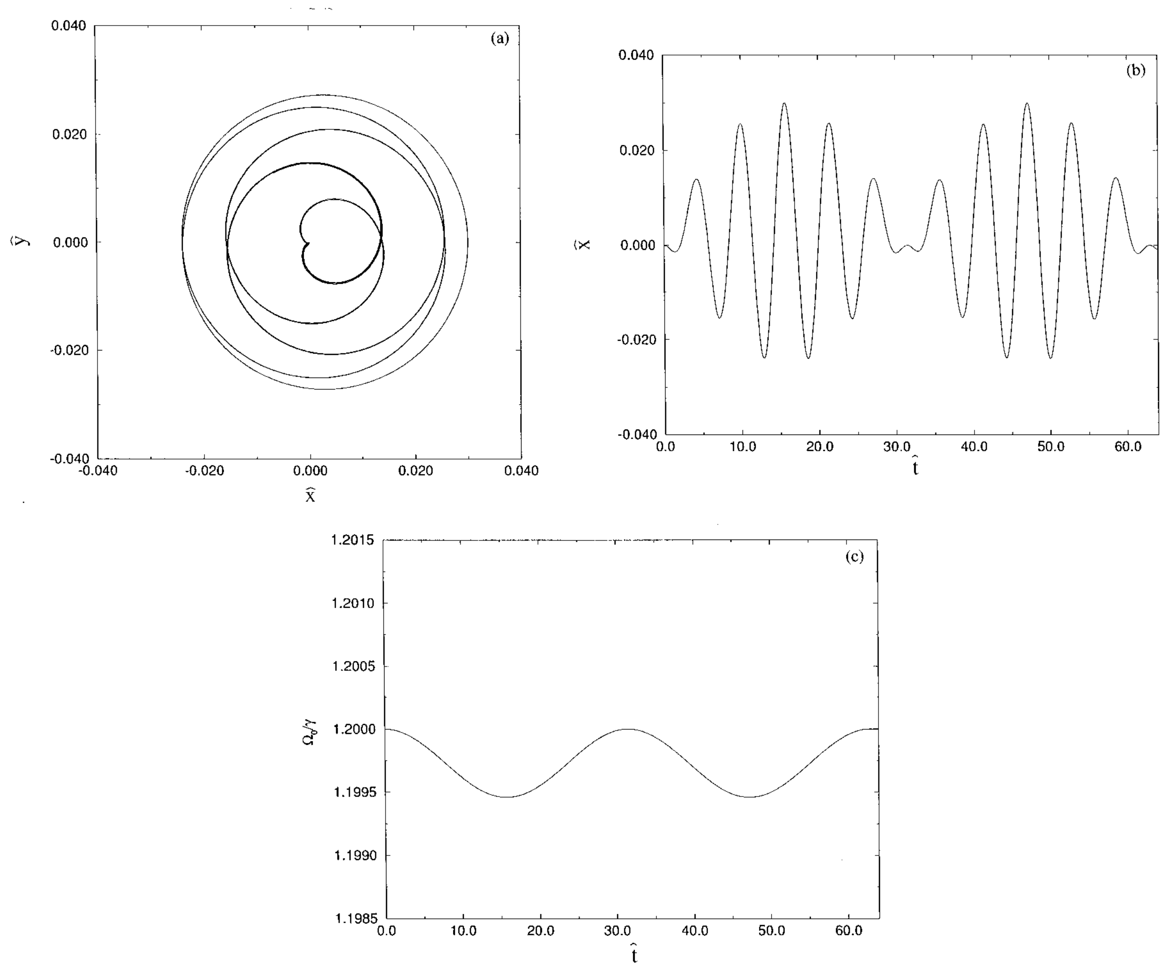

FIG. 2. (a) Trajectory of a particle in the $\hat{x}$-$\hat{y}$ plane in a case when the particle is initially at $\hat{x}_0=\hat{y}_0=0$ and at rest ($\gamma_0=1$ and $\Omega_0=1.2$) and when the resonance condition ($\Omega_0/\gamma=1$) is never reached. (b) $\hat{x}$ component of the charged particle in the same conditions as those of (a). (c) Evolution of Ω_0/γ versus time in the situation of (a).

Another constant of motion can be obtained using Noether's theorem [4,5], which says that if the Lagrangian is invariant under the infinitesimal transformation

$$t \to t + \varepsilon g(t,\mathbf{r}),$$
$$\mathbf{r} \to \mathbf{r} + \varepsilon \mathbf{u}(t,\mathbf{r}), \tag{5}$$

where ε is an infinitesimal, then a constant of motion is

$$\frac{\partial L}{\partial \mathbf{v}} \cdot \mathbf{u} + \left(L - \mathbf{v} \cdot \frac{\partial L}{\partial \mathbf{v}} \right) g, \tag{6}$$

where $L=-mc^2\sqrt{1-v^2/c^2}-e\mathbf{A}\cdot\mathbf{v}$ is the Lagrangian and $\mathbf{v}$ the velocity of the charged particle. It is simple to show that the Lagrangian of the system is invariant under the transformation

$$t \to t - \varepsilon/\omega_0, \quad x \to x + \varepsilon y, \quad y \to y - \varepsilon x. \tag{7}$$

Therefore, a third first integral is

$$C_3 = yP_x - xP_y + H/\omega_0. \tag{8}$$

It can be noticed that the first two constants are canonically conjugated

$$\left\{ C_1, \frac{C_2}{eB_0} \right\} = 1. \tag{9}$$

This last property will be used to reduce the dimension of the problem by choosing these two constants as new conjugated momentum and coordinate.

The dimensionless variables and parameters are now introduced

$$\hat{x} = x\,\frac{\omega_0}{c}, \quad \hat{y} = y\,\frac{\omega_0}{c}, \quad \hat{P}_{x,y} = \frac{P_{x,y}}{mc}, \quad \hat{t} = \omega_0 t,$$

$$\hat{H} = \gamma = \frac{H}{mc^2}, \quad a = \frac{eE_0}{mc\omega_0}, \quad \Omega_0 = \frac{eB_0}{m\omega_0}.$$

The new Hamiltonian is

$$\hat{H} = \left[\left(\hat{P}_x - a\,\sin\hat{t} - \frac{\Omega_0}{2}\,\hat{y} \right)^2 + \left(\hat{P}_y + a\,\cos\hat{t} + \frac{\Omega_0}{2}\,\hat{x} \right)^2 + 1 \right]^{1/2}. \tag{10}$$

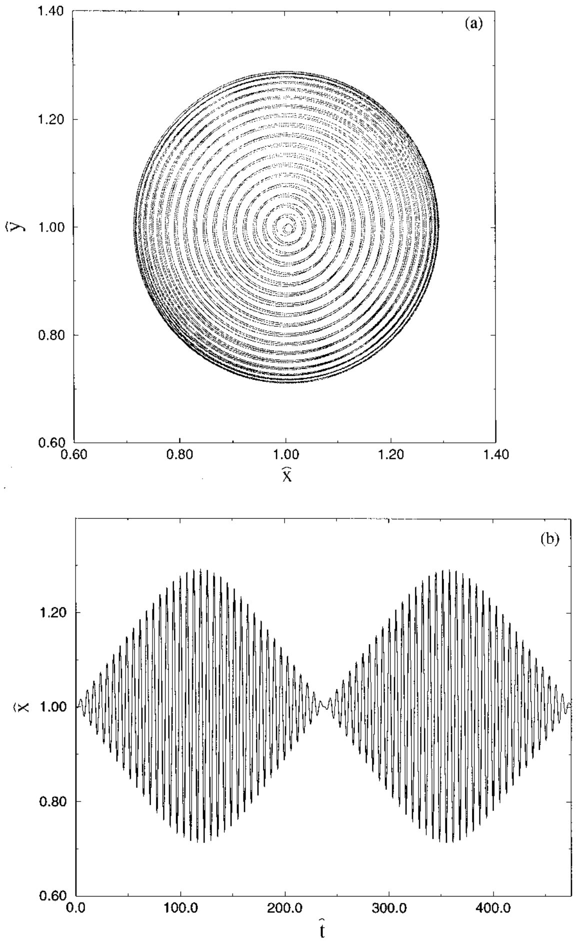

FIG. 3. (a) Trajectory of a charged particle initially resonant and at rest in the $\hat{x}$-$\hat{y}$ plane. $\hat{x}_0=\hat{y}_0=1$ and $a=3\times 10^{-3}$. (b) $\hat{x}$ component of the charged particle in the same conditions as those of (a).

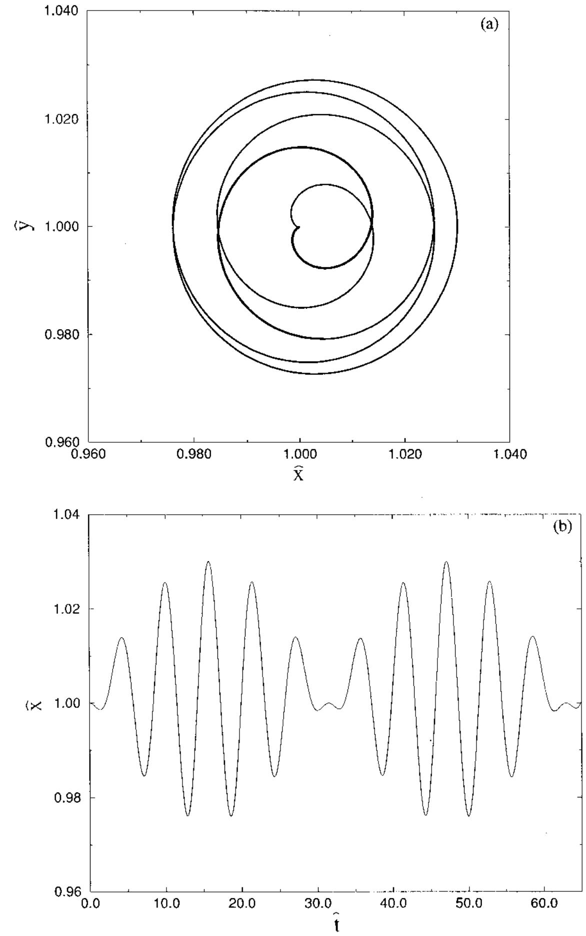

FIG. 4. (a) Trajectory of a particle initially at rest and nonresonant ($\Omega_0=1.2$). The initial position is the same as in the case of Fig. 3(a). (b) $\hat{x}$ component of the charged particle in the same conditions as those of (a).

The canonical equations are solved numerically using a fourth-order Runge-Kutta method. Figures 1(a), 2(a), 3(a), 4(a), and 5 show different types of trajectories. When the particle is initially at rest and a small ($a \ll 1$), it spirals outward and inward (Figs. 1–4). Different conditions are considered. Two situations are always compared in each case. The first is when a resonance condition ($\omega_0=eB_0/m\gamma$ or $\Omega_0/\gamma=1$) is satisfied (Figs. 1 and 3) and the second is when one is sufficiently far from any resonance (Figs. 2 and 4). When the initial energy is high and the electric field is low enough, the trajectories become almost circles; Fig. 5 shows such a trajectory in a case when the resonance condition is never satisfied. Some analytical insight from an approximate analytic solution of Hamilton's equations will be given to these numerical results in the following.

B. Demonstration of the integrability of the problem

Let us show that this problem can be described from a single degree of freedom time-dependent Hamiltonian. A first canonical transformation is introduced: $(\hat{x},\hat{y},\hat{P}_x,\hat{P}_y)\rightarrow(\tilde{x},\tilde{y},\tilde{P}_x,\tilde{P}_y)$, given the type-2 generating function [6]

$$F_2=\left(\tilde{P}_x-\frac{\Omega_0}{2}\,\hat{y}\right)\hat{x}+\tilde{P}_y\hat{y}. \tag{11}$$

This yields the canonical transformation

$$\hat{x}=\tilde{x},\quad \hat{y}=\tilde{y},\quad \hat{P}_x=\tilde{P}_x-\frac{\Omega_0}{2}\,\tilde{y},\quad \hat{P}_y=\tilde{P}_y-\frac{\Omega_0}{2}\,\tilde{x}. \tag{12}$$

In these variables C_1 and C_2 become

$$\tilde{C}_1=\tilde{P}_x,\quad \tilde{C}_2=\tilde{P}_y-\Omega_0\tilde{x}. \tag{13}$$

Then a second canonical transformation is introduced: $(\tilde{x},\tilde{y},\tilde{P}_x,\tilde{P}_y)\rightarrow(Q_1,Q_2,P_1,P_2)$, generated by

$$F_2=(P_2+\Omega_0\tilde{x})\tilde{y}+P_1\left(\tilde{x}+\frac{P_2}{\Omega_0}\right) \tag{14}$$

and yielding

$$\tilde{x}=Q_1-\frac{P_2}{\Omega_0},\quad \tilde{y}=Q_2-\frac{P_1}{\Omega_0},\quad \tilde{P}_x=\Omega_0 Q_2,\quad \tilde{P}_y=\Omega_0 Q_1. \tag{15}$$

The resulting transformation, which is a product of the two transformations, is given by

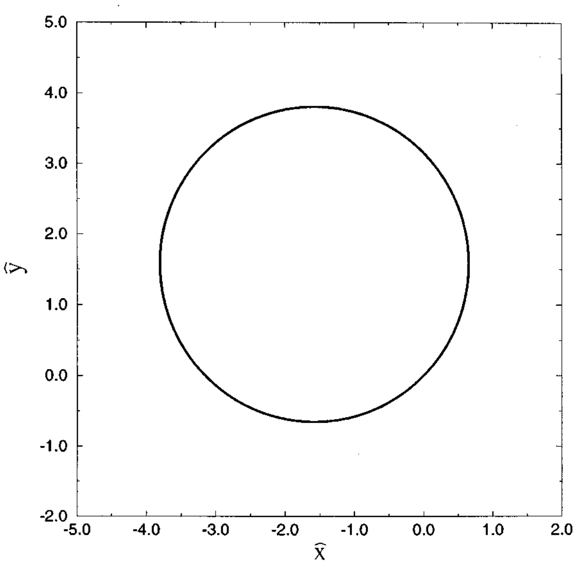

FIG. 5. Trajectory of an electron with a high initial energy in the $\hat{x}$-$\hat{y}$ plane (γ_0=4.57). Ω_0=2 and $a=3\times10^{-3}$.

$$\hat{x}=Q_1-\frac{P_2}{\Omega_0},$$

$$\hat{y}=Q_2-\frac{P_1}{\Omega_0},$$

$$\hat{P}_x=\tfrac{1}{2}(\Omega_0 Q_2+P_1),\tag{16}$$

$$\hat{P}_y=\tfrac{1}{2}(\Omega_0 Q_1+P_2).$$

In these variables, the Hamiltonian is

$$\mathcal{H}=[(P_1-a\sin\hat{t})^2+(\Omega_0 Q_1+a\cos\hat{t})^2+1]^{1/2}.\tag{17}$$

As expected, P_2 and Q_2 are cyclic variables. The Hamiltonian depends on time and has one degree of freedom. The new equations of Hamilton are

$$\dot{P}_1=-\frac{\Omega_0}{\gamma}(\Omega_0 Q_1+a\cos\hat{t}),\quad \dot{Q}_1=\frac{1}{\gamma}(P_1-a\sin\hat{t}).\tag{18}$$

The constant C_3 becomes

$$I=\mathcal{H}-\frac{P_1^2}{2\Omega_0}-\frac{\Omega_0}{2}Q_1^2.\tag{19}$$

The formal inversion of I with respect to P_1 provides

$$P_1=G(Q_1,I,\hat{t}),\tag{20}$$

where G is the reciprocal function of I. Introducing one equation of the Hamilton, we get

$$\dot{Q}_1=h(Q_1,I,\hat{t}),\tag{21}$$

which can be considered as a first-order differential equation with parameter I. In order to integrate Eq. (21), we look for an integrating factor $\alpha(Q_1,I,\hat{t})$ satisfying the equation

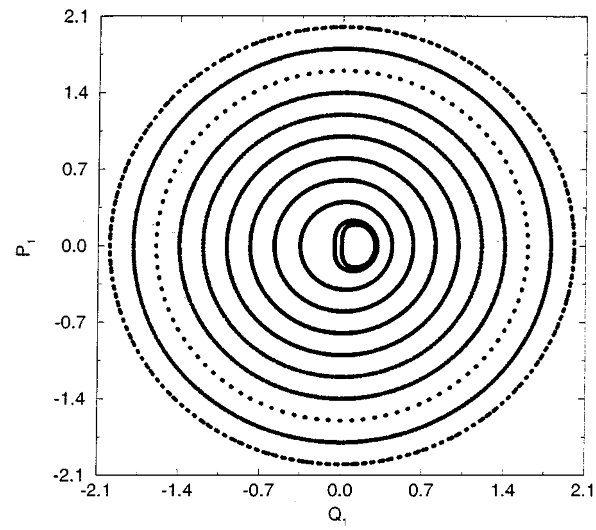

FIG. 6. Surface of section plots for some trajectories when $\gamma_0=\Omega_0=1$ and $a=3\times10^{-3}$.

$$\alpha_t+\alpha_{Q_1}h+\alpha h_{Q_1}=0,\tag{22}$$

where subscripts stand for partial derivatives. One can show that a solution to Eq. (22) is [7,8]

$$\alpha=G_I(Q_1,I,\hat{t})=[I_{P_1}(Q_1,P_1,\hat{t})]^{-1},\tag{23}$$

where $G_I=\partial G/\partial I$ and $I_{P_1}=\partial I/\partial P_1$. Then a second first integral in terms of $(Q_1,I,\hat{t})$ can be found for the one degree of freedom system. This integral has to satisfy

$$J_{Q_1}(Q_1,I,\hat{t})=G_I(Q_1,I,\hat{t}),$$
$$J_{\hat{t}}(Q_1,I,\hat{t})=-G_I(Q_1,I,\hat{t})h(Q_1,I,\hat{t}).\tag{24}$$

Integration leads to

$$J(Q_1,I,\hat{t})=\int_0^{Q_1}\frac{dQ_1'}{I_{P_1}(Q_1';P_1=G(Q_1',I,\hat{t});\hat{t})}-\int_0^{\hat{t}}\frac{\mathcal{H}_{P_1}(0;P_1=G(0,I,\hat{t}');\hat{t}')}{I_{P_1}(0;P_1=G(0,I,\hat{t}');\hat{t}')}\,d\hat{t}'.\tag{25}$$

Equation (25) shows that Q_1 can be derived formally as a function of time. Consequently, our system is integrable. Thus Liouville's theorem still holds [7,8] in the case of a one-dimensional time-dependent problem.

Poincaré maps were performed, drawing one point each time $\hat{t}=0$ mod(2π) (Fig. 6) [6]. Many initial conditions were tried. They always yielded smooth curves, which is in good agreement with the fact that the system is integrable.

C. Solution of the equations of Hamilton as a function of the particle energy: Approximate solution

Introducing the variables

$$\overline{Q_1}=Q_1+(a/\Omega_0)\cos\hat{t},\quad \overline{P_1}=P_1-a\sin\hat{t}\tag{26}$$

and the complex quantity $Z=\overline{P_1}+i\Omega_0\overline{Q_1}$, the equations of Hamilton [Eqs. (18)] are equivalent to

$$\dot{Z}=\frac{i\Omega_0 Z}{\sqrt{1+|Z|^2}}-a\ \exp(i\hat{t}), \tag{27}$$

which is the equation of a nonlinear oscillator submitted to an external force. The solution of this equation is

$$Z=A_0\exp i[\sigma(\hat{t})+\delta]-a\int_0^{\hat{t}}\exp i[\sigma(\hat{t})-\sigma(\tau)+\tau]d\tau, \tag{28}$$

with

$$\sigma(\hat{t})=\Omega_0\int_0^{\hat{t}}d\tau\ \gamma^{-1}(\tau). \tag{29}$$

A_0 and δ are real constants. Then

$$\begin{aligned} P_1&=A_0\cos[\sigma(\hat{t})+\delta]+a\ \sin\hat{t}\\ &\quad -a\int_0^{\hat{t}}\cos[\sigma(\hat{t})-\sigma(\tau)+\tau]d\tau,\\ Q_1&=\frac{A_0}{\Omega_0}\sin[\sigma(\hat{t})+\delta]-\frac{a}{\Omega_0}\cos\hat{t}\\ &\quad -\frac{a}{\Omega_0}\int_0^{\hat{t}}\sin[\sigma(\hat{t})-\sigma(\tau)+\tau]d\tau. \end{aligned} \tag{30}$$

The quantities A_0 and δ are determined so that at $\hat{t}=0$, $A_0^2=\gamma_0^2-1=\hat{p}_{x0}^2+\hat{p}_{y0}^2$ and $\tan\delta=\hat{p}_{y0}/\hat{p}_{x0}$ ($\hat{p}=p/mc$ and p is the momentum of the particle). The subscript 0 appended to variables γ and p refers to their initial value.

Our numerical results show that, when a is small and when γ_0 is close to unity, γ varies very little during a gyroperiod ($2\pi\dot{\gamma}/\Omega_0\ll 1$). It must be pointed out that considering a as a small quantity is experimentally realistic, especially for low-Q cavities. In any case, a is given by $a=(e/mc)(QP/\omega_0^3\varepsilon_0 V)^{1/2}$, where ε_0 is the permittivity of free space, V is the volume of the cavity, and P is its power loss. For a magnetron delivering 700 W and exciting a 2.5-GHz mode in a 1-liter resonant cavity, one has for electrons $a\approx 8.4\times 10^{-5}\sqrt{Q}$. When Q is 1–10^4, a is in the range 10^{-4}–10^{-2}. Because of this, the crudest possible approximation was performed; it is assumed that γ is a constant in the integrations that are in Eq. (28) or Eqs. (30). This leads to the approximate solution

$$\begin{aligned} P_1&=A_0\cos\left(\frac{\Omega_0}{\gamma}\hat{t}+\delta\right)+a\sin\hat{t}\\ &\quad -2a\frac{\sin\left[\left(1-\frac{\Omega_0}{\gamma}\right)\frac{\hat{t}}{2}\right]}{\left(1-\frac{\Omega_0}{\gamma}\right)}\cos\left[\left(1+\frac{\Omega_0}{\gamma}\right)\frac{\hat{t}}{2}\right],\\ Q_1&=\frac{A_0}{\Omega_0}\sin\left(\frac{\Omega_0}{\gamma}\hat{t}+\delta\right)-\frac{a}{\Omega_0}\cos\hat{t}\\ &\quad -\frac{2a}{\Omega_0}\frac{\sin\left[\left(1-\frac{\Omega_0}{\gamma}\right)\frac{\hat{t}}{2}\right]}{\left(1-\frac{\Omega_0}{\gamma}\right)}\sin\left[\left(1+\frac{\Omega_0}{\gamma}\right)\frac{\hat{t}}{2}\right]. \end{aligned} \tag{31}$$

This approximate solution can also be obtained by applying the multiple-time-scale method to Eq. (27) [10]. The number of time variables is extended from one variable $\hat{t}$ to three independent variables $\tau_0=\hat{t}$, $\tau_1=\varepsilon\hat{t}$, and $\tau_2=\varepsilon^2\hat{t}$, where $\varepsilon=a/\Omega_0$ is the small parameter. Z is expanded in ε according to

$$Z=Z^{(0)}+\varepsilon Z^{(1)}+g\varepsilon^2 Z^{(2)}. \tag{32}$$

We treat τ_0, τ_1, and τ_2 as independent variables and expand the time derivative as

$$\frac{d}{d\hat{t}}=\frac{\partial}{\partial\tau_0}+\varepsilon\frac{\partial}{\partial\tau_1}+\varepsilon^2\frac{\partial}{\partial\tau_2}. \tag{33}$$

γ is assumed to be a slowly varying quantity. One has to suppose it is a function of τ_2 only. We find, for $Z^{(0)}$,

$$Z^{(0)}=\overline{Z}(\tau_1,\tau_2)\exp\left[i\frac{\Omega_0}{\gamma(\tau_2)}\tau_0\right]. \tag{34}$$

In order to have a uniformly valid solution for $Z^{(1)}$, we use the freedom to remove any secular behavior to set

$$\frac{\partial\overline{Z}}{\partial\tau_1}=0. \tag{35}$$

The solution correct to order ε can be written

$$Z=Z_0\exp\left(i\frac{\Omega_0}{\gamma}\hat{t}\right)+i\frac{a\gamma}{(\gamma-\Omega_0)}\left[\exp(i\hat{t})-\exp\left(i\frac{\Omega_0}{\gamma}\hat{t}\right)\right], \tag{36}$$

where Z_0 is a complex constant. Setting $Z_0=A_0\exp(i\delta)$, Eq. (36) leads to the derivation of Eqs. (31) again. This second way to derive Eqs. (31) indicates how slow the variation of γ must be so that the approximate solution is a good one.

Figure 7(a) shows that when one remains far from resonance, there is excellent agreement between the exact and the approximate solution. Figure 7(b) shows that when a resonance condition is met ($\Omega_0/\gamma=1$), the agreement is good only for a short time compared to the time scale of the envelop evolution. In these two cases the approximate solution permits one to predict at least the aspect of the trajectory. It shows [Eqs. (31)] that when the particle is initially at rest, when $A_0=0$ ($\gamma_0=1$), P_1 and Q_1 result in a beating between two waves; this explains why trajectories spiral outward and inward. In this situation, when no resonance condition is met, it can be shown numerically that, roughly speaking, the exact trajectories are approached ‘‘correctly’’ by the approximate solution for a long time, as far as $a<0.1$. When the resonance condition is met, only the trend of the trajectories can be given when $a<10^{-2}$. For large values of γ_0 and small values of a ($A_0\gg a$), the trajectories are close to

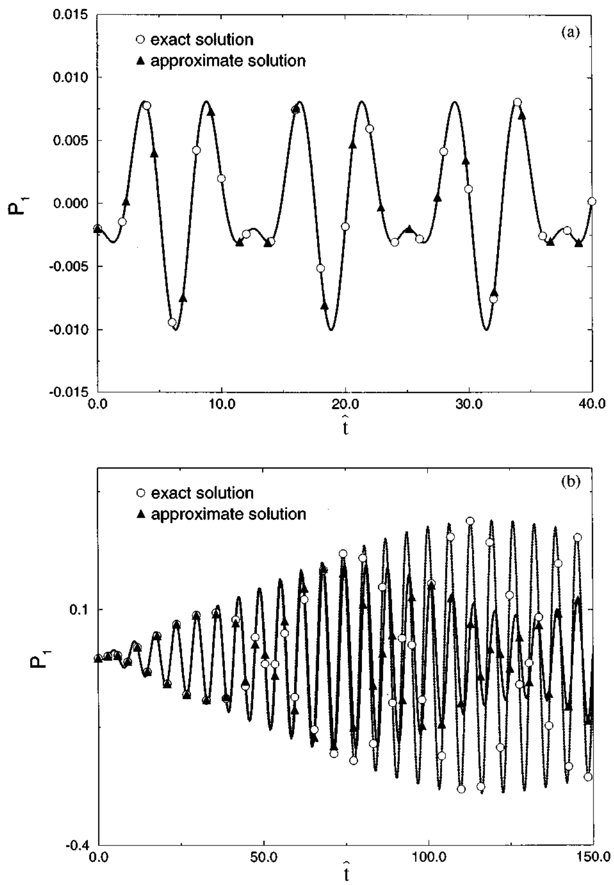

FIG. 7. (a) Comparison of the results obtained with the exact equations [Eqs. (18)] and the approximate solution [Eqs. (31)] in a case when the resonance condition is never verified. $\gamma_0=1$, $\Omega_0=1.5$, and $a=3\times10^{-3}$. (b) Comparison of the results obtained with the exact equations and the approximate solution in a case when the particle is initially resonant and at rest. $a=3\times10^{-3}$.

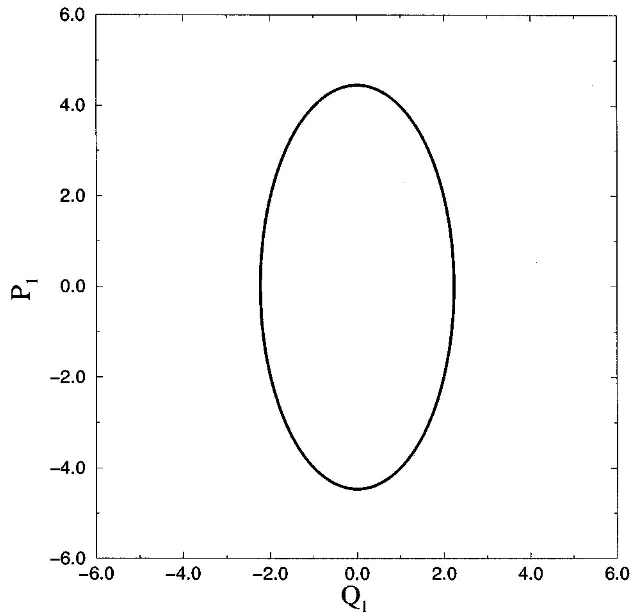

FIG. 8. Trajectory of a charged particle in the Q_1-P_1 plane. The same conditions as in the case described in Fig. 5 are considered.

ellipses in the Q_1-P_1 plane, as predicted by Eqs. (31) (Fig. 8). According to the canonical transformations [Eqs. (16)], they are almost circles in the $\hat{x}$-$\hat{y}$ plane (Fig. 5).

III. ENERGY OF THE PARTICLE

A. Differential equation for the energy

Taking the derivative of Eq. (17) with respect to time and using Eqs. (30), we obtain

$$\gamma\dot{\gamma}=-a\left\{A_0\cos[\sigma(\hat{t})-\hat{t}+\delta]-a\int_0^{\hat{t}}\cos[\sigma(\hat{t})-\sigma(\tau)+\tau-\hat{t}]d\tau\right\}. \tag{37}$$

This equation, multiplied by $\Omega_0/\gamma-1$ and integrated between 0 and $\hat{t}$, leads to

$$\Omega_0(\gamma-\gamma_0)-\frac{(\gamma^2-\gamma_0^2)}{2}-aA_0\sin\delta=-a\left\{A_0\sin[\sigma(\hat{t})-\hat{t}+\delta]-a\int_0^{\hat{t}}\sin[\sigma(\hat{t})-\sigma(\tau)+\tau-\hat{t}]d\tau\right\}. \tag{38}$$

Then Eq. (37) is differentiated with respect to time and Eq. (38), multiplied by $\Omega_0/\gamma-1$, is added to it. The resulting equation is multiplied by $\gamma\dot{\gamma}$ and integrated between 0 and $\hat{t}$. In this way, the following differential equation for the energy is derived:

$$\dot{\gamma}^2+\frac{\gamma^2}{4}-\Omega_0\gamma+R_0-\frac{\Gamma_0}{\gamma}-\frac{K_0}{\gamma^2}=0, \tag{39}$$

with

$$R_0=aA_0\sin\delta+\Omega_0^2+\Omega_0\gamma_0-\frac{\gamma_0^2}{2}-a^2, \tag{40}$$

$$\Gamma_0=2\Omega_0 aA_0\sin\delta+2\Omega_0^2\gamma_0-\Omega_0\gamma_0^2, \tag{41}$$

and

$$K_0=a^2A_0^2\cos^2\delta-\Gamma_0\gamma_0+R_0\gamma_0^2-\Omega_0\gamma_0^3+\frac{\gamma_0^4}{4}. \tag{42}$$

This result is in good agreement with the one obtained by Roberts and Buchsbaum [1]. $\dot{\gamma}$ can be solved numerically as a function of γ. Some results are shown in Fig. 9. Equation (39) describes motion in a one-dimensional potential. It admits a solution that gives time in terms of a sum of elliptic integrals of the first and the third type [11]. The inversion

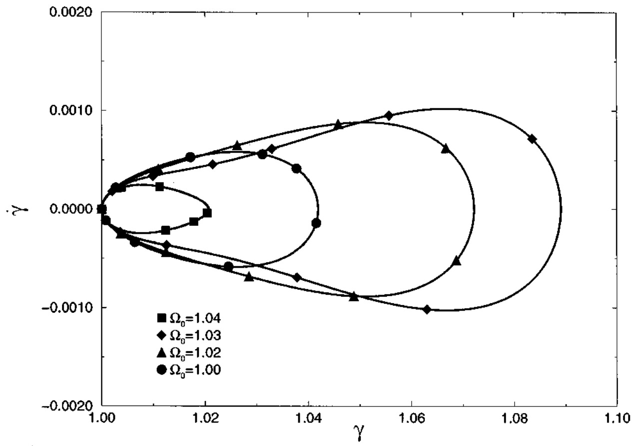

FIG. 9. Trajectories in the $\dot{\gamma}$-γ phase space for $\gamma_0=1$, $a=3\times10^{-3}$, and different values of Ω_0.

process, which consist of deriving γ as a function of time, does not lead to any practical result. As a consequence, it is more interesting to study qualitatively the behavior of γ in its phase space. Still, the fact that a solution of Eq. (39) exists permits, with the help of Eqs. (30), one to prove a second time that this problem is integrable.

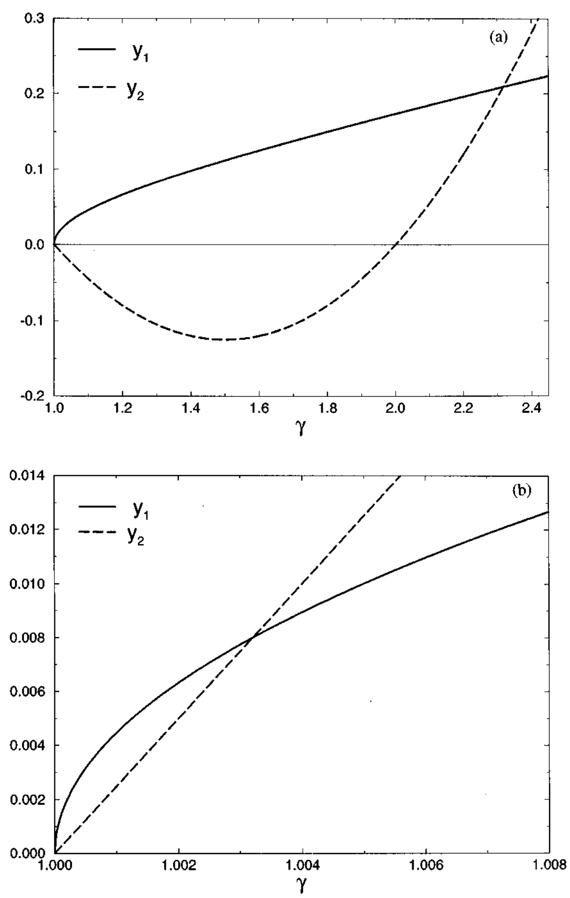

FIG. 10. Functions y_1 and y_2 versus γ for (a) $\Omega_0=1.5$ and $a=0.1$ and (b) $\Omega_0=-1.5$ and $a=0.1$.

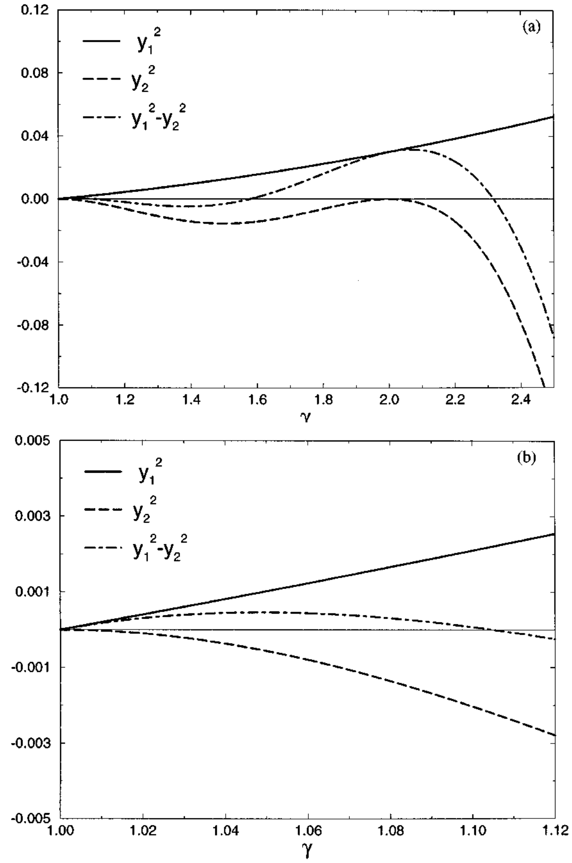

FIG. 11. $\gamma^2\dot{\gamma}^2$ versus γ as the result of the addition of y_1^2 and $-y_2^2$. $\Omega_0=1.5$ and $a=0.1$. (b) Magnification of (a) at low energy.

B. Phase-space analysis

Equation (39) can also be written

$$\gamma^2\dot{\gamma}^2=a^2(\gamma^2-1)-\left\{aA_0\sin\delta+(\gamma-\gamma_0)\left[\left(\frac{\gamma+\gamma_0}{2}\right)-\Omega_0\right]\right\}^2. \tag{43}$$

This expression is more tractable in the phase space $(\gamma,\dot{\gamma})$ than Eq. (39).

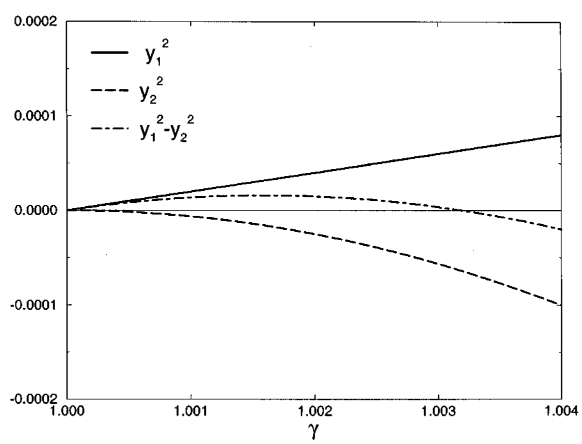

FIG. 12. Evolution of $\gamma^2\dot{\gamma}^2$ at low energy when $\Omega_0=-1.5$ and $a=0.1$.

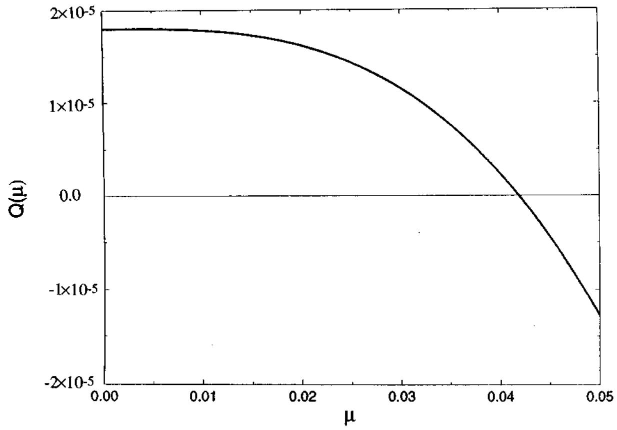

FIG. 13. $Q(\mu)$ versus μ when $a=3\times10^{-3}$ (thick solid line).

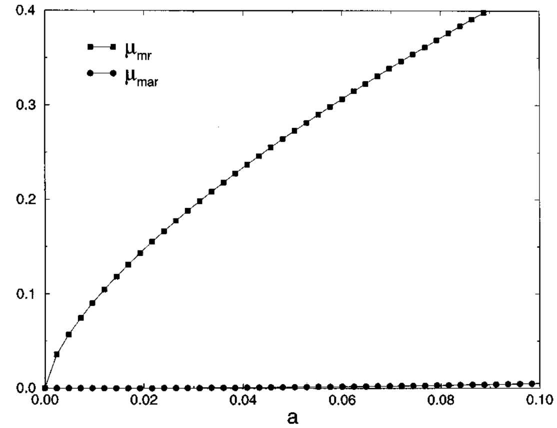

FIG. 15. Comparison of the maximum normalized kinetic energies reached when the particle is initially resonant μ_{mr} and ''antiresonant'' μ_{mar}. $\gamma_0=1$.

Let us consider the case when the particle is initially nonresonant and at rest ($\gamma_0=1$ and $\Omega_0\neq1$). We set $y_1=[a^2(\gamma^2-1)]^{1/2}$ and $y_2=\frac{1}{2}(\gamma-1)[\gamma+1-2\Omega_0]$ [Figs. 10(a) and 10(b)]. In Figs. 11(a) and 11(b), in the case $\Omega_0>1$, the square of the second quantity is substracted from the square of the first. The same procedure can be done when $\Omega_0<1$ (Fig. 12). As $\gamma^2\dot{\gamma}^2$ has to be positive, γ remains in the finite domain including γ_0 and oscillates between two values. This is in good agreement with the fact that Eq. (39) cannot be satisfied by too high a value of γ.

The interesting case when the particle is initially resonant and at rest is now considered ($\gamma_0=\Omega_0=1$). Setting $\gamma=1+\mu$, Eq. (43) becomes

$$\gamma^2\dot{\gamma}^2=\mu\left[a^2(\mu+2)-\frac{\mu^3}{4}\right]. \tag{44}$$

As $\mu\geqslant0$, the sign of the third-order polynomial $Q(\mu)=a^2(\mu+2)-\mu^3/4$ has to be positive. In any case, $Q(\mu)$ has only one real positive root. Three situations are possible: $Q(\mu)$ has only one real root when $a<\sqrt{27}/2$ (Fig. 13); it can have either three real roots or two (with one double) when $a\geqslant\sqrt{27}/2$; as $Q(\mu)$ is positive between $\mu=0$ and its positive root μ_{mr}, the kinetic energy (μ) oscillates between these two values. Assuming that a is very small ($a\ll1$), which is an experimentally interesting situation, then $Q(\mu)$ has only one real root. Equation (44) yields

$$\mu_{mr}\approx2a^{2/3}. \tag{45}$$

In this situation ($\gamma_0=\Omega_0=1$), Eq. (39) was solved numerically for different values of a. The maximum value of γ reached by the particle is compared in Fig. 14 to the one obtained through Eq. (45). Very good agreement between the two results is observed.

Another interesting situation is the case when the particle is initially ''antiresonant'' and at rest ($\gamma_0=1$ and $\Omega_0=-1$). Then

$$\gamma^2\dot{\gamma}^2=\mu\left(-\frac{\mu^3}{4}-2\mu^2+(a^2-4)\mu+2a^2\right). \tag{46}$$

The third-order polynomial $T(\mu)=-(\mu^3/4)-2\mu^2+(a^2-4)\mu+2a^2$ has only one positive root when a is a sufficiently small quantity. In this case, the maximum value for the normalized kinetic energy is approximately given by

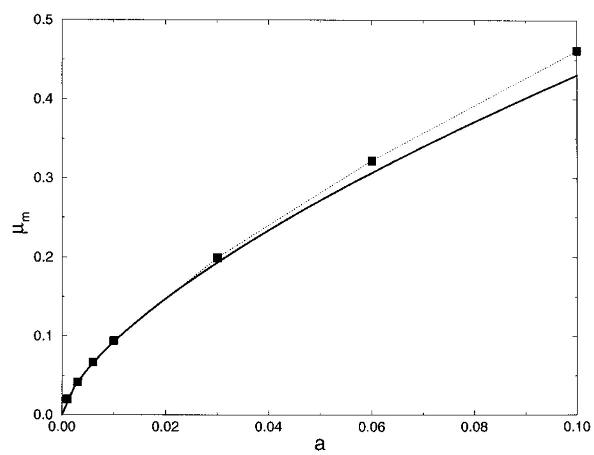

FIG. 14. Comparison between the maximum normalized kinetic energy reached by the particle calculated through Eq. (39) (full line) and Eq. (45) (full squares and dashed line). $\Omega_0=\gamma_0=1$.

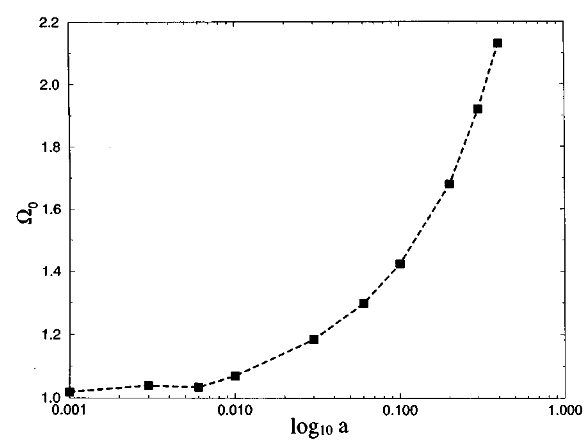

FIG. 16. Value of the magnetic field leading to the maximum energy for the charged particle versus a. $\gamma_0=1$.

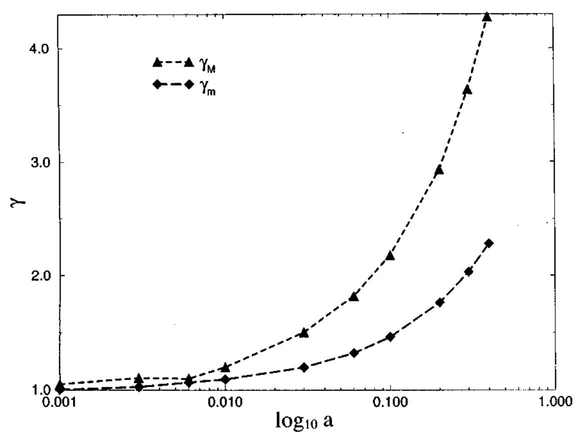

FIG. 17. Maximum possible energy for the particle (γ_M) versus a, when the particle is initially at rest, compared to the one obtained when the particle is initially resonant and at rest (γ_m).

$$\mu_{m\mathrm{ar}} \approx \frac{a^2}{2}. \tag{47}$$

A comparison between the maximum values of μ obtained through Eqs. (45) and (47) is shown in Fig. 15. It points out how important it is to take the magnetic field in the right direction.

When the particle is initially at rest, the maximum energy is not reached when it is initially resonant. Figure 16 shows the values of the parameter Ω_0 for which the maximum energy is reached, for different a in the range (1×10^{-3})–0.4. An approximate expression for Ω_0 obtained for a third-order polynomial fit to the data yields

$$\Omega_0 \approx 1.0205 + 5.0753a - 11.1858a^2 + 13.6444a^3. \tag{48}$$

Figure 17 shows the corresponding maximum energy γ_M, compared to the maximum energy γ_m reached when the particle is initially resonant.

IV. CONCLUSION

Using the Hamiltonian formalism, we have reduced the problem of relativistic motion of a charged particle in a constant homogeneous magnetic field and a transverse rotating electric field to a time-dependent problem with a single degree of freedom. Noether's theorem was used to find a constant of motion for the system. Then a second integral is derived. It gives an alternative way of showing that this problem is integrable. The Hamiltonian formalism also gives insight into the problem in the sense that it enables the derivation of a simple approximate solution for the equations of motion, which leads to the prediction of at least the aspect of the trajectories.

An equation for the energy was obtained and studied in the phase plane. When the charged particle is initially at rest, it shows that the energy oscillates between two values. Tractable approximate expressions for the maximum attainable energy are obtained for low values of parameter a (which is an experimentally interesting situation), when the electron is initially resonant and antiresonant. Finally, an approximate expression is given for the value of the magnetic field (Ω_0) for which the maximum energy is reached.

ACKNOWLEDGMENTS

The authors wish to thank Professor J. M. Buzzi, Professor J. Virmont, Professor P. Choi, and Dr. S. Bouquet for very valuable discussions.

APPENDIX

When the motion is considered to be nonrelativistic, the two components of the equation of motion may be written as

$$m\,\frac{dv_x}{dt} = -e(E_x + v_y B_0), \quad m\,\frac{dv_y}{dt} = -e(E_y - v_x B_0), \tag{A1}$$

where v_i is a component of the charged particle velocity. In matrix notation this set of equations reads

$$m\,\frac{d\mathbf{v}}{dt} = -e(\mathbf{E} + eB_0\mathbf{J}\cdot\mathbf{v}), \tag{A2}$$

where $\mathbf{v}=(v_x, v_y)$, $\mathbf{J}=\begin{pmatrix} 0 & 1 \\ -1 & 0 \end{pmatrix}$, and $\mathbf{E}=(E_x, E_y)$. The solution of this equation can be given in terms of

$$\mathbf{G}(t) = \exp(\beta t \mathbf{J}), \tag{A3}$$

with $\beta = -(e/m)B_0$,

$$\mathbf{v}(t) = \mathbf{G}(t)\cdot\mathbf{v}_0 - \frac{e}{m}\int_0^t \mathbf{G}(t-s)\cdot\mathbf{E}(s)ds. \tag{A4}$$

This equation enables the derivation of x and y by a simple quadrature. This points out how simple it is to show that the problem is integrable in the nonrelativistic limit. In order to simplify the calculation of the velocity, one can verify that [12]

$$\mathbf{G}(t) = \mathbf{I}\cos(\beta t) + \mathbf{J}\sin(\beta t), \tag{A5}$$

where I is the matrix identity. Then, at resonance (when $\omega_0 = eB_0/m$), Eq. (A4) leads easily to the expression for the kinetic energy [1,13]

$$E_c = \frac{1}{2}\,m|v|^2 = \frac{1}{2}\,mv_0^2 - eE_0 v_{0x} t + \frac{e^2E_0^2}{2m}\,t^2. \tag{A6}$$

The energy of the particle increases indefinitely and does not oscillate as in the relativistic case. The reason is that the gyrofrequency is a function of the velocity of the charged particle when the relativistic equations of motion are considered. The particle cannot remain resonant. This is the main difference from the relativistic case. Other differences concern trajectories. For instance, when a particle is initially at rest and resonant it spirals outward indefinitely.

[1] C. S. Roberts and S. J. Buchsbaum, Phys. Rev. **135**, A381 (1964).
[2] A. Hakkenberg and M. P. H. Weenink, Physica **30**, 2147 (1964).
[3] H. R. Jory and A. W. Trivelpiece, J. Appl. Phys. **39**, 3053 (1968).
[4] H. Goldstein, *Classical Mechanics*, 2nd ed. (Addison-Wesley, New York, 1980).
[5] R. D. Jones, Phys. Fluids **24**, 564 (1981).
[6] A. J. Lichtenberg and M. A. Liebermann, *Regular and Stochastic Motion* (Springer-Verlag, Berlin, 1983).
[7] S. Bouquet and A. Dewisme, *Nonlinear Evolution Equations and Dynamical Systems*, edited by M. Boiti, L. Martina, and F. Pempinelli (World Scientific, Singapore, 1992).
[8] A. Dewisme and S. Bouquet, J. Math. Phys. **34**, 997 (1993).
[9] V. I. Arnold, *Dynamical Systems* (Springer-Verlag, Berlin, 1988), Vol. III; S. N. Rasband, *Dynamics* (Wiley, New York, 1983).
[10] R. C. Davidson, *Methods in Nonlinear Plasma Theory* (Academic, New York, 1972).
[11] P. F. Byrd and M. D. Friedman, *Handbook of Elliptic Integrals for Engineers and Physicists* (Springer-Verlag, Berlin, 1954).
[12] R. Dautray and J. L. Lions, *Analyse Mathématique et Calcul Numérique pour les Sciences et les Techniques* (Masson, Paris, 1985).
[13] J.-L. Delcroix and A. Bers, *Physique des Plasmas* (InterEditions/CNRS Editions, Paris, 1994).